Supporting Information

Roland et al. 10.1073/pnas.1707050114

SI Results

VMHC. We quantified the changes in VMHC between precallosotomy and postcallosotomy states by anatomically defined regions in the complete and partial groups. Primary sensorimotor: complete – $t(15) = -6.300$, $P < 0.001$; partial – $t(5) = -4.388$, $P = 0.043$. Primary vision: complete – $t(15) = -4.747$, $P < 0.001$; partial – $t(5) = -0.532$, $P = 0.618$. Frontal: complete – $t(15) = -6.445$, $P < 0.001$; partial – $t(5) = -2.736$, $P = 0.041$. Parietal: complete – $t(15) = -5.712$, $P < 0.001$; partial – $t(5) = -2.388$, $P = 0.063$. Occipital: complete – $t(15) = -5.627$, $P < 0.001$; partial – $t(5) = -1.257$, $P = 0.264$. Temporal: complete – $t(15) = -3.365$, $P = 0.004$; partial – $t(5) = -1.251$, $P = 0.266$.

To further quantify the magnitude of changes by complete and partial groups, we calculated the Cohen's d between precallosotomy and postcallosotomy results for each anatomic region by group. Primary sensorimotor: complete 2.40, partial 2.49; primary vision: complete 1.72, partial 0.30; frontal: complete 2.62, partial 1.48; parietal: complete 2.33, partial: 1.35; occipital: complete 1.94, partial 0.57; temporal: complete 1.38, partial 1.88. The difference in Cohen's d between groups for each region informs us on the magnitude of effect by respective callosotomy. Sorting this difference from greatest to least confirms that the primary vision area shows the greatest difference in FC changes between complete and partial callosotomy (1.41), followed by occipital (1.37), frontal (1.14), parietal (0.99), temporal (0.51), and primary sensorimotor (0.08).

Similar analysis was performed by RSN regions of interest (Fig. S5) as defined by an average RSN parcellation map (Fig. S6). These results demonstrate the frontal and parietal regions observed the greatest reduction in VMHC after complete callosotomy, and the primary vision region was most preserved after partial callosotomy. We measured VMHC in seeds placed in select locations including brain regions not directly connected by CC fibers (Fig. S7). Seeds in the frontal, temporal, and parietal areas exemplify areas disconnected by complete callosotomy. However, the sensorimotor and primary vision areas show VMHC decreases similar to the cerebellum and putamen, areas not expected to be disconnected by callosotomy. The thalamus showed the least decrease in VMHC after complete callosotomy. The seed coordinates in MNI-152 space are as follows: frontal –75, 79, –63; temporal –85, 50, –66; parietal –76, 40, –45; sensorimotor –72, 49, –45; primary vision –69, 26, –64; cerebellum –75, 39, –76; putamen –71, 63, –66; thalamus –69, 53, –61.

Follow-Up Imaging at Delayed Time Interval. The first individual (Fig. 5*A*) underwent partial callosotomy at age 2 y (subject 1, Table S1). Repeat imaging was performed 2 y later. The delayed (2-y postcallosotomy) study showed FC largely similar to the results obtained 1 d after the initial procedure.

The second individual (Fig. 5*B*) underwent complete callosotomy at age 13 y (subject 19, Table S1). Repeat imaging was performed 7 y later. The delayed study showed an unusually large shared variance, as observed in the greater magnitude correlations widely seen in the delayed FC matrix. This feature most likely reflects that this subject uniquely was able to tolerate nonsedated MRI, hence, was studied while awake.

The third individual (Fig. 5*C*) had an acute worsening of seizure frequency at age 15 y, leading to a state of epileptic encephalopathy treated by complete callosotomy. The 1-d postoperative study revealed a markedly disorganized pattern similar to that previously reported in another case of epileptic encephalopathy (19). Repeat imaging, performed 2 y later, showed improved intrahemispheric organization (in association with dramatic improvement in seizure control) but very little interhemispheric FC. Due to acute presentation with epileptic encephalopathy before intervention, preoperative data were not reported and this subject was not included in any of the above group analysis. Propofol was used for sedation at the 1-d and 2-y postcallosotomy time points.

We computed the elementwise correlation coefficient between the precallosotomy, postcallosotomy, and delayed follow-up FC matrices to quantify the change between each time point. These correlations demonstrate a greater similarly between intrahemispheric FC between each time point compared with a least similarity for interhemispheric FC between precallosotomy and immediate postcallosotomy for each subject (Fig. 5*A* – Pre vs. Post: Right 0.40, Left 0.35, Inter 0.05; Post vs. Delay: Right 0.57, Left 0.53, Inter 0.23; Fig. 5*B* – Pre vs. Post: Right 0.57, Left 0.43, Inter 0.23; Post vs. Delay: Right 0.47, Left 0.54, Inter 0.35; Fig. 5*C* – Post vs. Delayed: Right 0.23, Left 0.19, Inter 0.08).

SI Discussion

Patients undergoing corpus callosotomy all have severe, medically refractory epilepsy with nonfocal onset, typically involving drop attacks. These individuals often have significant cognitive deficits. As the profile of pediatric epilepsy is very broad, there is significant variability in medication usage, seizure semiology, and cognitive function. For this reason, we do not attempt to compare the organization of FC to typically developing individuals. Instead, we compare postcallosotomy to precallosotomy FC within individual. Hence, we caution that the results obtained any particular individual in this cohort may be atypical.

Corpus callosotomy is better tolerated at a young age. Therefore, we are unable to study human adults both before and after callosotomy. The individuals in our study were 2–18 y old, which age range spans a significant portion of the postnatal developmental period. Therefore, we expect that our inferences regarding structure-function relations apply generally.

All individuals contributing to the present results were free of gross anatomic lesions on diagnostic imaging. However, the existence of a severe seizure disorder implies that some pathology must be present, notwithstanding no imaging correlate. Emerging evidence has identified various FC abnormalities in different forms of epilepsy (45–47). However, these abnormalities are subtle and, therefore, are unlikely to compromise the present main inferences.

Individuals who are candidates for corpus callosotomy often cannot hold still in a MRI scanner owing to cognitive disability, either as a consequence of long-term epilepsy or comorbid pathology. These individuals cannot be scanned without sedation. Sedation clearly reduces head motion artifact, which otherwise would preclude useful rs-fMRI (48). Fortunately, RSNs are robust to propofol sedation, which is commonly used in ambulatory studies (49). Our study used similar sedation before and after callosotomy (Table S1). However, the requirement for sedation presents an obstacle to clinically not indicated MRI, as sedation is not entirely without risk. This circumstance at least partially accounts for the sparse representation of delayed follow-up rs-fMRI data (ultimately obtained in only 3 of 16 patients).

Apart from the challenges of acquiring rs-fMRI in the callosotomy population, the clinical imaging protocol under which the data were acquired necessitated modifying our approach to image registration. Specifically, precallosotomy T1w scanning was performed with gadolinium contrast, which interferes with

image registration to a conventional T1-weighted atlas template. Hence, atlas registration of the functional data was computed using a newly created T2-weighted template (Fig. S2). Despite these technical difficulties, our methodology produced good image alignment across subjects before and after callosotomy (Fig. 1).

SI Methods

Corpus Callosotomy Subjects. Inclusion criteria included medically refractory epilepsy and no identifiable lesion or structural abnormality (e.g., arachnoid cyst, cortical dysplasia). Patients presenting with acute epileptic encephalopathy requiring urgent intervention were not studied (see Table S1 for demographics). The decision to perform complete or partial callosotomy was decided on the basis of clinical criteria alone by an interdisciplinary epilepsy team consisting of neurosurgeons, neurologists, neuroradiologists, and clinical psychologists. Partial callosotomy is preferred in higher functioning individuals in whom the risk of disconnection syndrome is thought to be high. However, the decision generally is balanced by the consideration that better seizure control is achieved with complete callosotomy (43).

We attempted to contact all subjects for follow-up imaging following the initial postoperative recovery period. This agenda is complicated because many callosotomy patients cannot tolerate nonsedated MRI, whereas the risk of sedation for nonclinically indicated imaging is not easily justified. Therefore, the present study includes only three individuals who returned for follow-up, one of whom was scanned while awake (Fig. 5*B*). One follow-up scan was aborted when the patient refused to enter the MRI.

Callosotomy Procedure. Corpus callosotomy was performed following a standard clinical protocol via open craniotomy and microsurgical technique, as previously described (43). In brief, the head is rigidly fixed in place and frameless stereotactic image guidance is used for neuronavigation. Access is achieved with a coronal or "trap-door" incision and a parasagittal craniotomy eccentric to the right. The craniotomy flap extends ∼4 cm in front of and 2 cm behind the coronal suture and is 4 cm wide. An interhemispheric approach is taken in the plane between the falx and right cerebral hemisphere. An operative microscope is used to enter the avascular midline between the pericallosal arteries. Section of the CC proceeds through a combination of aspiration and bipolar electrocautery.

Image Before and After Processing. Resting-state preprocessing followed standard methodology as has been previously published (44). In brief, this included correction for asynchronous slice acquisition, normalized slice intensity to mode 1,000, and correction of interframe head motion. BOLD data were resampled to 3-mm cubic voxels before time-series correlation analysis. We temporally low-pass filtered the BOLD time series at <0.1 Hz and spatially smoothed it with a 6-mm full-width half-max Gaussian kernel. Nuisance variables included parameters derived from rigid body head motion correction, bilateral lateral ventricle, and white-matter regions of noninterest. The global signal was not included to eliminate any ambiguity in the interpretation of observed findings (50). Following nuisance regression, frame censoring was computed using the temporal derivative of root-mean-square frame-to-frame BOLD signal change across voxels (DVARS). Frames exceeding DVARS = 0.5% were excluded from the FC analyses (48). The DVARS values representing artifact timeseries are plotted in Fig. S8 to demonstrate the very little motion present in our sedated subjects.

The CC was manually traced in the midsagittal using the precallosotomy and postcallosotomy T1w structural images for individuals that underwent partial callosotomy. The ratio of CC area remaining postcallosotomy to precallosotomy was calculated. The similarity of interhemispheric FC between precallosotomy and postcallosotomy was calculated as described in *FC Matrices*. There was not a significant relationship between callosotomy ratio and prepost interhemispheric FC (Pearson correlation $r = 0.52$, $P = 0.29$). This suggests the little variance observed in structural disconnection among patients undergoing partial callosotomy did not correlate with the difference in FC.

In fMRI generally, atlas registration of the functional data are achieved by composition of transforms connecting the EPI, T2w, and T1w images. Conventionally, the T1w structural image is registered to a T1w atlas-representative template. We did not use the preoperative T1w image for atlas registration because it included gadolinium contrast. The postoperative T1w images were also not used for atlas registration because the introduced anatomical deformations, albeit minor, theoretically could have compromised the results. To overcome these barriers, atlas registration was computed via T2w atlas-representative template generated using a previously published strategy (51). Thus, the preoperative T2w (12-parameter affine) was registered to this template. The remaining images then were registered to the preoperative T2w, both within and across sessions (Fig. S2).

We used Matlab 2015b for further data analysis. For statistical tests of precallosotomy and postcallosotomy measures within subject we used paired *t* tests, and for comparison between complete and partial or intrahemispheric and interhemispheric measures, we used the two-sample *t* test. All tests were two-tailed and used a predefined significance threshold of $\alpha = 0.05$.

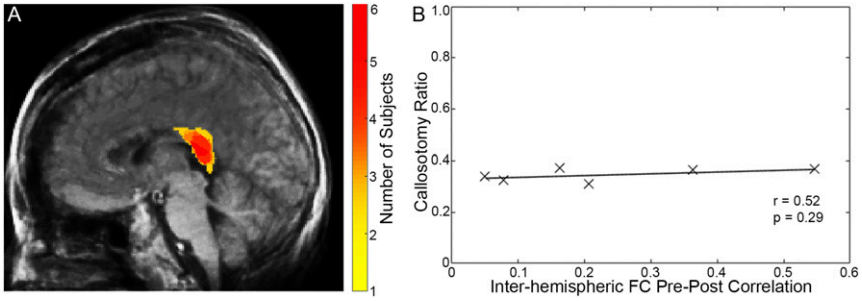

Fig. S1. Residual CC after partial callosotomy. (*A*) An overlap analysis of the posterior portion of the CC that was spared by the partial callosotomy procedure. The heat map identifies the number of subjects where overlap occurs for each voxel at $x = -4$. The size and shape of an individual's CC is variable, but the sparing of the splenium was consistent in the partial callosotomy procedure. (*B*) The proportion of callosum sectioned (posterior third including the splenium) was consistent across partial subjects and did not show a significant association with similarity of interhemispheric FC precallosotomy and postcallosotomy.

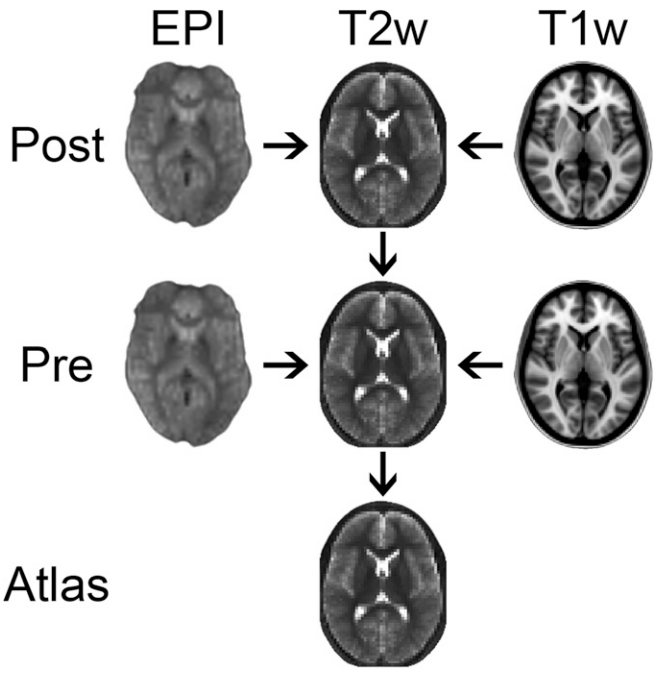

Fig. S2. Image alignment procedure. Precallosotomy T2w images were registered to a T2w atlas representative target. Then postcallosotomy T2w was aligned to the precallosotomy T2w. T1w and EPI images were aligned to the respective T2w image by cross-modal registration.

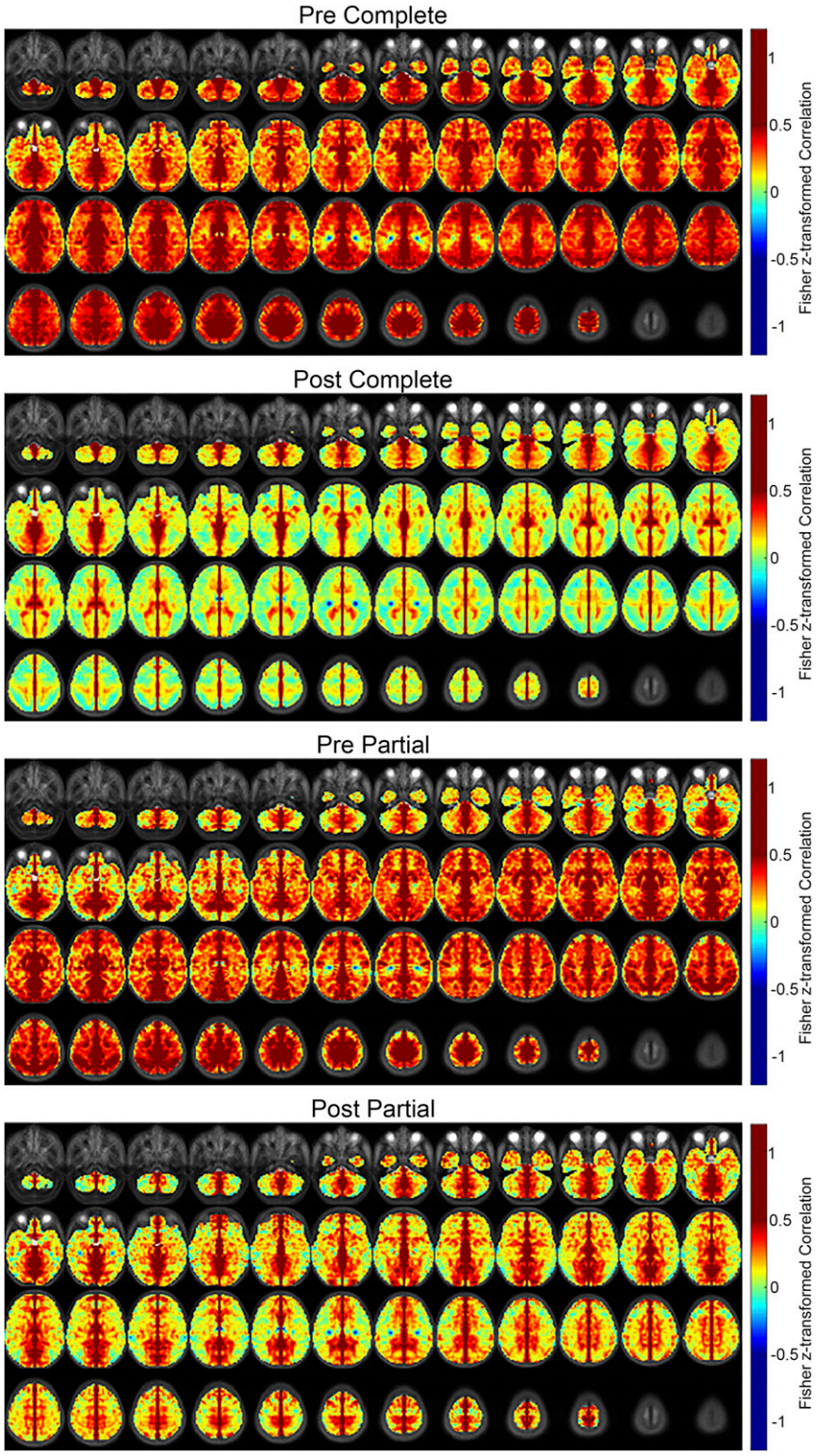

Fig. S3. Full VMHC maps. Mean VMHC maps for all slices are displayed in a similar format to the exemplar images in Fig. 4*A*.

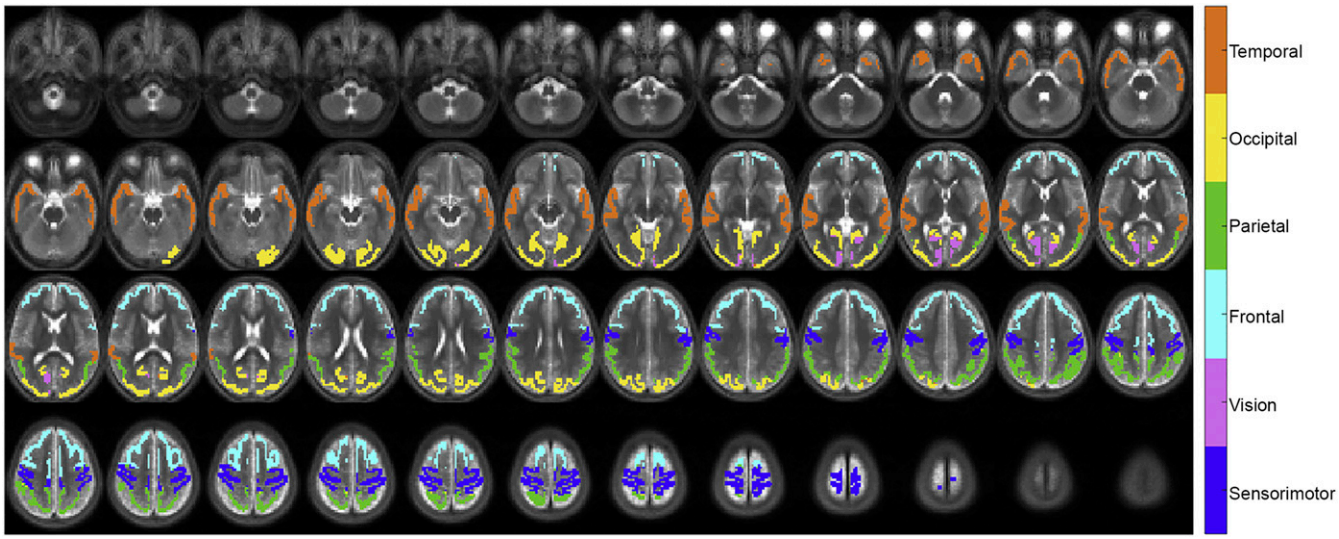

Fig. S4. Anatomic labels by Brodmann area. The anatomic labels used for sampling VMHC precallosotomy and postcallosotomy are overlaid on the T2w atlas representative image. Anatomic labels include primary sensorimotor (blue), primary vision (purple), frontal (cyan), parietal (green), occipital (yellow), and temporal (orange) cortical areas.

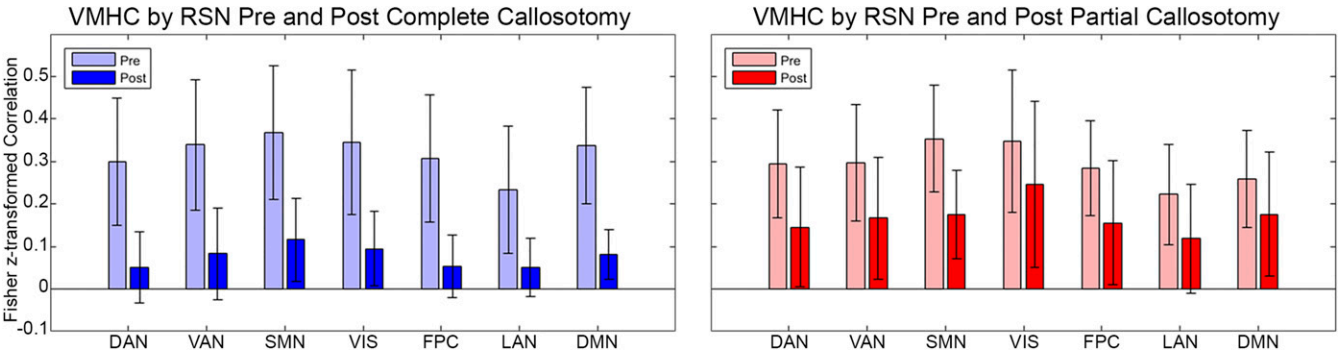

Fig. S5. Change in VMHC by RSN. Mean (and 95% confidence interval) VMHC precallosotomy and postcallosotomy by RSN are displayed in bar graph format for complete and partial callosotomy. Voxels were assigned to one of seven RSNs including DAN, DMN, FPC, LAN, SMN, VAN, and VIS. Membership to each RSN was determined by a previously published group average winner-take-all map (Fig. S6).

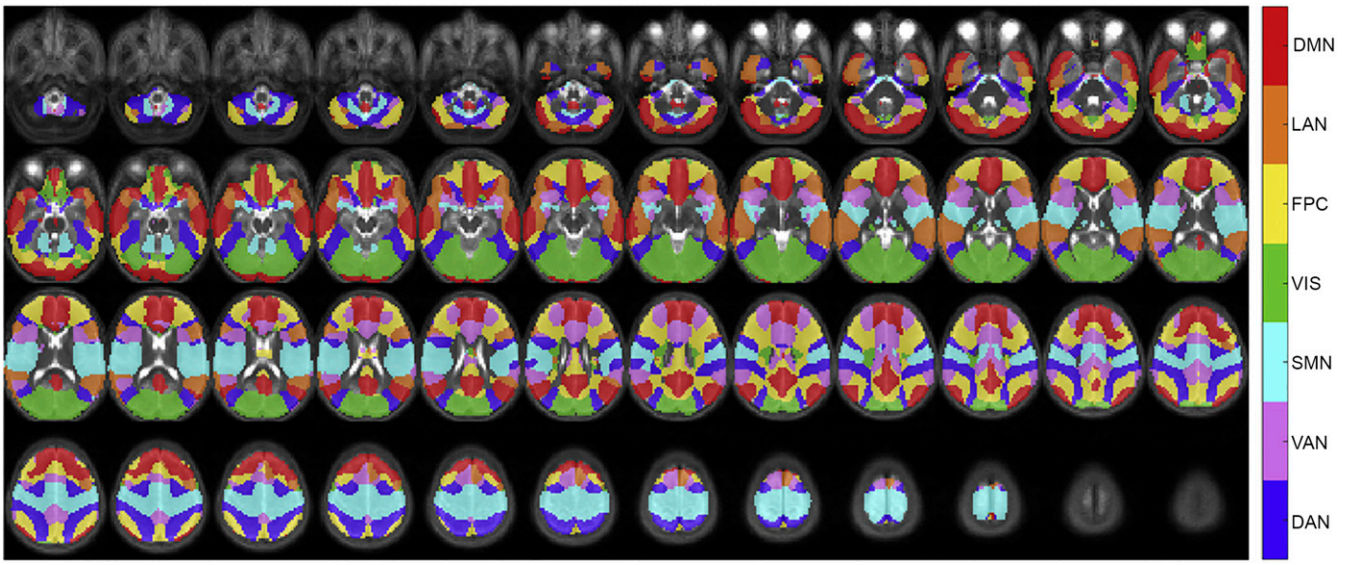

Fig. S6. RSN labels. The RSN labels used for sampling VMHC precallosotomy and postcallosotomy overlaid on the T2w atlas representative image. RSN labels include DAN, blue; DMN, red; FPC, yellow; LAN, orange; SMN, cyan; VAN, purple; VIS, green.

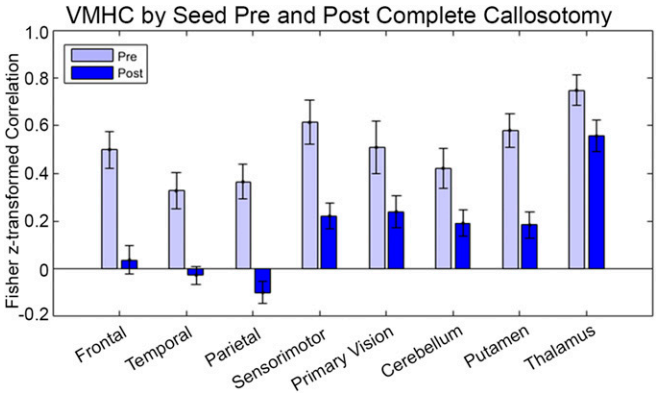

Fig. S7. Change in VMHC including regions not disconnected. VMHC is examined by placing a seed in select regions before and after complete callosotomy. The cerebellum, putamen, and thalamus represent regions without direct connections via the CC. The cerebellum and putamen show similar degree of decrease in VMHC compared with sensorimotor and primary vision areas but less so than more associative cortical areas such as the frontal, temporal, and parietal areas. The thalamus showed the least change after complete callosotomy. Error bars represent 95% confidence intervals.

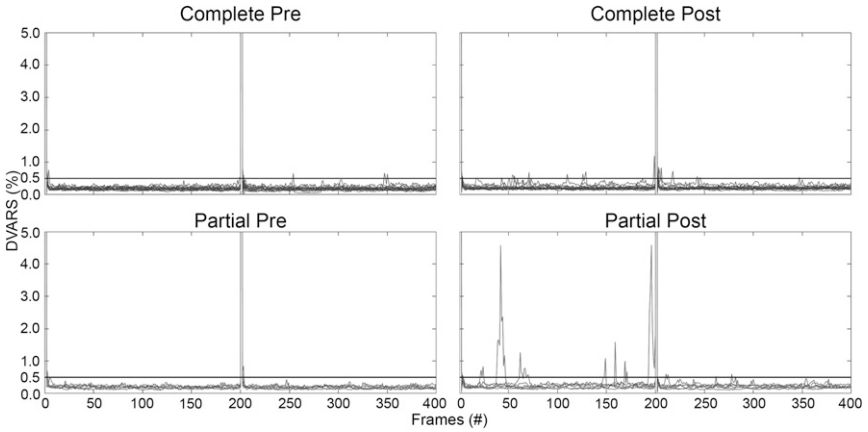

Fig. S8. DVARS movement data. The DVARS are plotted for all subjects by complete and partial groups precallosotomy and postcallosotomy. The horizontal bold line marks the 0.5% DVARS threshold at which frames where censored for motion. Four hundred frames total were collected in two runs of 200 frames each for all sessions. Very little movement is noted across all subjects owing to the effect of sedation used for both sessions.

Table S1. Subject characteristics

Subject	Callosotomy	Age, y	Sex	Sedation preprocedure	Sedation postprocedure	Antiepileptic drugs
1	Partial	2.3	F	Propofol	Propofol	Levetiracetam, Rufinamide/Banzel, Clobazam
2	Complete	3.2	M	Propofol	Dexmedetomidine	Clobazam, Felbamate, Valproic acid
3	Complete	4.9	F	Propofol	Propofol	Felbamate, Phenobarbital
4	Complete	5.1	M	Propofol	Pentobarbitol	Clobazam, Phenobarbital
5	Partial	5.5	M	Propofol	Dexmedetomidine	Zonisamide, Carbamazepine
6	Complete	6.1	M	Propofol	Propofol	Levetiracetam, Lamotrigine, Ethosuximide
7	Complete	7.6	F	Propofol	Propofol	Felbamate
8	Complete	7.8	M	Propofol	Propofol	Lamotrigine, Methsuximide
9	Complete	7.9	F	Propofol	Remifentanil	Felbamate, Topiramate, Valproic acid
10	Partial	9.3	M	Propofol	Propofol	Felbamate, Topiramate, Clobazam
11	Complete	10.7	F	Propofol	Propofol	Clonazepam, Felbamate
12	Complete	11.7	M	Propofol	Pentobarbitol	Clobazam, Felbamate, Levetiracetam, Zonisamide
13	Complete	12.1	M	Propofol	Ativan	Lacosamide, Levetiracetam, Zonisamide
14	Partial	12.1	M	Propofol	Propofol	Valproate, Felbamate, Clonazepam, Methsuximide
15	Complete	12.4	M	Propofol	Propofol	Lamotrigine, Levetiracetam, Valproic acid
16	Partial	12.5	M	Propofol	Propofol	Levetiracetam, Felbamate, Rufinamide
17	Complete	12.8	M	Propofol	Propofol	Citalopram, Rufinamide, Topiramate
18	Partial	13.4	M	Propofol	Propofol	Clonazepam, Levocarnitine
19	Complete	13.4	M	Propofol	Pentobarbitol	Felbamate, Lamotrigine, Topiramate
20	Complete	15.1	M	Propofol	Dexmedetomidine	Clobazam, Felbamate, Valproic acid
21	Complete	15.6	F	Propofol	Propofol	Felbamate, Topiramate, Valproic Acid
22	Complete	17.2	M	Propofol	Propofol	Clobazam, Lacosamide

F, female; M, male.